Ciprofibrate attenuates airway remodeling in cigarette smoke-exposed rats

Qian Ke[a], Lin Yang[a], Qinghua Cui[b], Wenqi Diao[a], Youyi Zhang[c,d,e,f], Ming Xu[c,d,e,f,g,*,1], Bei He[a,**,1]

[a] Department of Respiratory Medicine, Peking University Third Hospital, Beijing, China
[b] Department of Biomedical Informatics, Department of Physiology and Pathophysiology, Center for Noncoding RNA Medicine, MOE Key Lab of Cardiovascular Sciences, School of Basic Medical Sciences, Peking University, Beijing, China
[c] Department of Cardiology and Institute of Vascular Medicine, Peking University Third Hospital, Beijing, China
[d] NHC Key Laboratory of Cardiovascular Molecular Biology and Regulatory Peptides, Beijing, China
[e] Key Laboratory of Molecular Cardiovascular Science, Ministry of Education, Beijing, China
[f] Beijing Key Laboratory of Cardiovascular Receptors Research. Beijing, China
[g] Department of Integration of Chinese and Western Medicine, School of Basic Medical Sciences, Peking University, Beijing, China

ARTICLE INFO

ABSTRACT

Airway remodeling is a key pathological lesion in chronic obstructive pulmonary disease (COPD), and it leads to poorly reversible airway obstruction. Current pharmacological interventions are ineffective at controlling airway remodeling. To address this issue, we queried the Connectivity Map (cMap) database to screen for drug candidates that had the potential to dilate the bronchus and inhibit airway smooth muscle (ASM) proliferation. We identified ciprofibrate as a drug candidate. Ciprofibrate inhibited cigarette smoke extract-induced rat ASM cell contraction and proliferation *in vitro*. We exposed Sprague-Dawley (SD) rats to clean air or cigarette smoke (CS) and treated the rats with ciprofibrate. Ciprofibrate improved pulmonary function, inhibited airway hypercontraction, and ameliorated morphological small airway remodeling, including airway smooth muscle proliferation, in CS-exposed rats. Ciprofibrate also significantly reduced IL-1β, IL-12p70, IL-17A and IL-18 expression, which are related to airway remodeling, in the sera of CS-exposed rats. These findings indicate that ciprofibrate could attenuate airway remodeling in CS-exposed rats.

1. Introduction

Chronic obstructive pulmonary disease (COPD) remains a leading cause of morbidity and mortality worldwide, and cigarette smoke is the predominant risk factor for COPD. Airway remodeling is a key pathological lesion in COPD, and it leads to poorly reversible airway obstruction (Barnes et al., 2015). The current therapy for airway remodeling in COPD is principally directed towards the amelioration of bronchoconstriction and airway inflammation using bronchodilators and glucocorticosteroids, respectively (Rabe and Watz, 2017). Notably, patients with airway remodeling in COPD are poorly controlled with the use of these drugs (Dekkers et al., 2013; Jones et al., 2016; Lahousse et al., 2016). This poor response emphasizes the need for the development of novel or repurposed drugs for airway remodeling in COPD treatment.

Airway remodeling is an intractable issue in COPD, and it is characterized by airway hypercontraction, airway smooth muscle (ASM) proliferation and airway fibrosis (Jones et al., 2016). Bronchial dilation and restraint of airway smooth muscle proliferation are important treatment targets in airway remodeling of COPD (Rabe and Watz, 2017). Active protein kinase A catalytic subunit C-alpha (PKA-Cα) catalysis of substrate phosphorylation mediates the functional antagonism of pro-contractile signaling in ASM (Pera and Penn, 2014). Cyclin D1 is a critical regulator of cell cycle progression. Cigarette smoke extract (CSE) increases ASM cyclin D1 expression and induces ASM proliferation in COPD (Pera et al., 2010; Xu et al., 2012). Therefore, the upregulation of PKA-Cα (*PRKACA*) and the downregulation of cyclin D1 (*CCND1*) may be potential therapeutic targets for airway remodeling in COPD and lead to bronchial dilation and the inhibition of ASM proliferation.

Drug repurposing is a strategy to identify new uses for approved or investigational drugs that are outside the scope of the original medical indication (Pushpakom et al., 2018). The repurposing of 'old' drugs is gradually becoming an attractive proposition because it involves the

use of less risky compounds with potentially lower overall development costs and shorter development timelines. Connectivity Map (cMap) information can be used as a proxy phenotypic screen for a large quantity of compounds, and it has been successfully applied for drug repurposing predictions in many disease conditions (Lamb et al., 2006; Qu and Rajpal, 2012). The cMap database exploits the transcriptome and uses gene expression profiling as a common 'language' to connect biology, chemistry and clinical conditions to discover disease-gene-drug connections.

We used the cMap database to repurpose potential drug candidates to attenuate CS-induced airway hypercontraction and ASM proliferation based on the upregulation of *PRKACA* and the downregulation of *CCND1*. We used literature mining to identify drugs that relaxed smooth muscles and inhibited cell proliferation and selected ciprofibrate as a drug candidate for further verification. Ciprofibrate, a peroxisome proliferator-activated receptor α (PPAR-α) agonist, is an effective treatment for three main types of atherogenic hyperlipoproteinemia: type IIa hypercholesterolemia, type IIb combined hyperlipidemia, and type IV hypertriglyceridemia in clinical (Li et al., 2018; Turpin and Bruckert, 1996). Moreover, it also plays a critical role in inhibiting vascular smooth muscle cell proliferation, regulating vascular tone and the inflammatory response in cardiovascular diseases (Li et al., 2018). PPAR-α has been shown to exert a potent anti-inflammatory activity in lung inflammatory diseases including acute lung injury, asthma and lung fibrosis (Banno et al., 2018; Belvisi and Mitchell, 2009; Cuzzocrea, 2006). So far, no information is available on the role of PPAR-α activation in ASM contraction and proliferation. It's unclear whether ciprofibrate attenuated airway remodeling in COPD. We investigated the effect of ciprofibrate on CSE-induced rat airway smooth muscle cell contraction and proliferation *in vitro* and assessed the efficacy of ciprofibrate on debilitating airway remodeling in CS-exposed rats. These findings may provide more direct experimental evidence and new ideas for COPD drug development.

2. Materials and methods

2.1. Connectivity map (cMap) analysis

The cMap database is a publicly available resource of transcriptional profiles induced by existing drugs. We used cMap to identify potential compounds that could reverse airway remodeling through COPD-associated genes. The database contains more than 7000 genome-wide transcriptomes from cultured human cells treated with 1309 bioactive compounds. *PRKACA* and *CCND1* genes were mapped into Affymetrix platform HG-U133A probe set IDs and used as input for cMap to query compounds that upregulated *PRKACA* and downregulated *CCND1*. The cut-off for the up/down regulation was a fold-change value of 2.0.

2.2. Primary rat airway smooth muscle cell (ASMC) culture

The trachea and main bronchi from Sprague-Dawley rats were carefully dissected and rinsed in phosphate buffer saline (PBS). The epithelium and serosa were carefully stripped using fine forceps and a surgical blade and cut into 1-mm pieces in culture plate. Cells were cultured in Dulbecco's Modified Essential Media (DMEM, Thermo Fisher Scientific, Waltham, MA, USA) supplemented with 20% fetal bovine serum (FBS) and 100 g/mL penicillin and 100 IU/mL streptomycin. Cells were grown at 37 °C in the presence of 5% CO_2. Primary rat ASMC emerged in approximately 7 days.

2.3. Cigarette smoke extract (CSE) preparation

CSE was prepared by bubbling smoke from five cigarettes (1R1; Derby Cigarettes, tar = 10 mg, cotinine = 0.9 mg, CO = 12 mg per cigarette, Wuhu Cigarette Inc., Anhui, China) through 10 mL of FBS-free DMEM supplemented with penicillin and streptomycin at a rate of

5 min/cigarette (Pera et al., 2010; Xu et al., 2012). The smoked medium was then sterile filtered through a 0.22 μm filter. The obtained solution represented 100% strength. The 100% CSE was freshly generated for each experiment, and diluted to final working concentration and used within 30 min. Cell viability was detected with different concentrations of CSE (0%, 0.25%, 0.50%, 1%, 2%, 4%) by using Cell Counting Kit-8 (CCK-8; Dojindo, Japan) to determine the optimum experimental concentration.

2.4. Collagen gel contraction assay

The concentration of the rat ASMC suspension was adjusted to 3×10^5/mL after trypsin digestion. A volume of 557 μL of the cell suspension was mixed with 333 μL of rat tail collagen type I (3 mg/ml, Thermo Fisher Scientific, Waltham, MA, USA), 100 μL of 10 × PBS and 10 μL of 1 M NaOH immediately (pH = 7.40). The resultant mixture (7.5×10^4 cells per well in 500 μL) was added to each well of a 24-well plate, and the formation of a collagen gel was induced via incubation at 37 °C under 5% CO_2 for 30 min. Freshly prepared collagen matrices were overlaid with DMEM containing 10% FBS and incubated for 48 h to allow the mechanical load to develop. Gel surface images were captured using a digital camera, and the contraction of the gel was evaluated by measurement of the surface area using ImageJ software (NIH, Bethesda, MD, USA). Data are expressed as the collagen contraction area percentage of the original gel size.

2.5. Western blotting

Total protein was extracted from rat ASMC using cold Radio Immunoprecipitation Assay (RIPA) buffer. The protein concentration in cell lysates was determined using a Pierce BCA protein assay kit (Pierce, Rockford, IL, USA). Proteins (30 μg) were loaded onto a 10% Sodium dodecyl sulfate (SDS) polyacrylamide gel and electrophoretically transferred to nitrocellulose membranes (Pall, Port Washington, USA). Membranes were incubated with antibodies according to the manufacturer's protocol. Immunolabeled bands were visualized using the SuperSignal West Pico chemiluminescence kit (Thermo Fisher Scientific). Autoradiographs were quantitated by densitometry using Image J software. Bands were normalized to GAPDH (1:20000, Abcam, Cambridge, UK) expression. The primary antibody was a cyclin D1 rabbit mAb (1:2000, Abcam).

2.6. Animals and experimental protocol

The Ethics Committee of Peking University Health Science Center approved all *in vivo* manipulations (permit No: LA2019004), and animal experiments were performed in accordance with the committee's animal care. Thirty-two male Sprague-Dawley rats (7 weeks old) were supplied by Beijing Vital River Laboratory and bred in-house. A CS-induced airway remodeling and COPD-like changes model was produced as described previously (Zhou et al., 2014a,b). Thirty-two rats were randomly divided into four groups for the challenge (n = 8 each): exposure to clean air or cigarette smoke (CS) for 28 weeks. Whole-body CS exposure involved use of the BUXCO animal CS-exposure system (DSI, USA) that provided smoke generated from commercial cigarettes (1R1; Derby Cigarettes, tar = 10 mg, cotinine = 0.9 mg, CO = 12 mg per cigarette, Wuhu Cigarette Inc., Anhui, China). The equivalent of 20 cigarettes' inhalation was administered over 2 h, followed by a 4-h recovery; this was repeated twice a day, 6 days/week. Rats were treated with ciprofibrate (10 mg/kg, Selleck, USA) (Herbert et al., 1999; Tzeng et al., 2015) or vehicle (1% carboxymethylcellulose sodium) once daily for 4 weeks from the 25th week of exposure. Ciprofibrate was administered 1 h before smoke exposure. All rats were euthanized after 28 weeks.

2.7. Pulmonary function testing

Pulmonary function tests were performed using the AniRes 2005 lung function meter (Peking Biolab Tech Company, Beijing, China), according to the manufacturer's instructions (Yue et al., 2017). The equipment was calibrated before use. Briefly, rats were anesthetized with 1% sodium pentobarbital (0.4 mg/100 g, intraperitoneal injection) prior to surgery. An endotracheal tube was inserted into the rats and connected to the outlet of a ventilator. After 30 normal respiratory cycles, the peak expiratory flow (PEF) and maximal mid-expiratory flow curve (MMF) were examined and recorded.

2.8. Contractile function of isolated tracheal segment smooth muscle

Rats were euthanized with 1% sodium pentobarbital (0.4 mg/100 g, intraperitoneal injection), and intact tracheae were quickly dissected and cleaned of connective tissues. Isolated trachea with eight cartilage rings was transferred to an organ bath containing a Krebs-Henseleit buffer solution maintained at 37℃, as previously described (Guo et al., 2014). Resting tension was adjusted stepwise to reach 0.5 g, and the tissue was stabilized for 1 h. Tracheal force contractions in response to increasing logarithmic-graded doses of acetylcholine were recorded using an isometric transducer connected to the PowerLab system (ADInstruments, Australia).

2.9. Histopathological analysis

The left lung tissue was embedded in paraffin and processed for standard hematoxylin-eosin and Masson-Goldner trichrome staining. Images were viewed under a DM2500 optical microscope (Leica Microsystems, Wetzlar, Germany) before any measurements, and a pathologist who was blinded to treatment analyzed the tissue. The pathological changes in the small airways were assessed using inflammation scores as described by Cosio et al. (1978). Three random microscope fields in which the bronchiole diameters were < 200 μm (shortest path/lumen diameter ≥ 0.7) were used to measure the bronchiole basement membrane perimeter (Pbm), airway wall area and collagen area. Total bronchiole wall area and collagen area around bronchioles were normalized to the Pbm (Reinhardt et al., 2005). The wall area/total bronchiole area (MA%) was also calculated.

2.10. Immunohistochemistry

After paraformaldehyde fixation, 5-mm paraffin-embedded lung tissues underwent immunohistochemical staining. The primary antibody for α-smooth muscle actin (α-SMA) was a mouse polyclonal anti-α-SMA (1:10000, Boster Biological Technology, Beijing, China). Sections were incubated at 4℃ overnight and incubated with the secondary antibody horseradish peroxidase-conjugated goat anti-mouse IgG (PV-6002; ZSGB-Bio, Beijing, China) for 30 min. Immunoreactivity was visualized with a Diaminobenzidine Detection System kit (ZLI-9018; ZSGB-Bio) for 45 s, and sections were counterstained with Mayer's hematoxylin. Negative controls for nonspecific binding omitted the primary antibody. The α-SMA staining area of the bronchioles was normalized to the Pbm in airways less than 200 μm in diameter.

2.11. Cytokine detection

The concentrations of cytokines (IL-1β, IL-12p70, IL-17A, IL-18, IL-33 and TNFα) were determined using the LEGENDplex Multi-analyte Flow Assay Kits (BioLegend, San Diego, CA, USA). The serum of rats was collected, and 25 μL of the supernatant was used for the assays, following the manufacturer's instructions. The data were analyzed using LEGENDplex Data Analysis Software (BioLegend).

2.12. Statistical analysis

All statistical analyses were performed using Statistical Package for the Social Sciences 18.0 software (Armonk, NY, USA). Data are presented as box-plots showing the medians and 25th and 75th percentiles and whiskers showing the 10th and 90th percentiles or the means ± standard error of the mean (SEM). In parametric data, ANOVA was used to analyze the differences among groups if data were determined to be normal distribution. For parametric data with unequal variances, ANOVA with Games-Howell post-hoc test was used. For non-parametric data, a Kruskal–Wallis ANOVA combined with post-hoc Dunn's multiple comparison test was performed when more than 2 groups were evaluated. Differences were considered significant at $P < 0.05$.

3. Results

3.1. The cMap-predicted drug candidate ciprofibrate attenuated airway remodeling

We used the cMap database to repurpose potential drug candidates that dilated the bronchus and inhibited airway smooth muscle proliferation (Table S1). Mepenzolate bromide, fulvestrant and raloxifene attenuate cigarette smoke-induced emphysema and airway remodeling (Tam et al., 2016; Tanaka et al., 2013), which suggest that the cMap predictions were reliable. Previous studies showed ciprofibrate relaxed vascular smooth muscle and restrained hepatoblastoma cell line HepG2 proliferation (Clemencet et al., 2005; Mujumdar et al., 2002), which were confirmed by literature mining. Therefore, we chose ciprofibrate for further cellular experiments to verify its potential to dilate airway smooth muscle cell (ASMC) and inhibit ASMC proliferation (Fig. 1A).

A collagen gel contraction assay was performed to determine whether ciprofibrate affected ASMC contractile function. Primary rat ASM cell viability was more than 98% when stimulated with cigarette smoke extract (CSE) not more than 1% (Fig. S1). CSE promoted ASMC contraction in a dose-dependent manner ($^{***}P < 0.001$, Figure S2). Ciprofibrate reduced CSE-induced ASMC contraction ($^{###}P < 0.001$, Fig. 1B). We found that CSE promoted the expression of cyclin D1 in rat ASMC in time-dependent and dose-dependent manners. ($^{**}P < 0.01$, $^{***}P < 0.001$, Figure S3). Ciprofibrate significantly decreased CSE-induced cyclin D1 expression in rat ASMC ($^{#}P < 0.05$, $^{###}P < 0.001$, Fig. 1C). These data suggest that ciprofibrate inhibited CSE-induced ASMC contraction and proliferation *in vitro*.

3.2. Ciprofibrate ameliorated lung function in cigarette smoke-exposed rats

Airway remodeling in COPD generally causes an irreversible loss of lung function in COPD (Barnes et al., 2015). We established a long-term CS-exposure rat model to induce airway remodeling and COPD-like changes and evaluated the effects of ciprofibrate on pulmonary function (Fig. 2A). Rats exposed to CS for 28 weeks without ciprofibrate showed a significant decrease in the peak expiratory flow (PEF) and maximal mid-expiratory flow curve (MMF) compared to the clean air-exposed group without ciprofibrate (Fig. 2B and C). The PEF increased 3.40% in the CS-exposed group treated with ciprofibrate compared to the CS-exposed group without ciprofibrate (44.68 ± 1.72 ml/s *vs.* 43.21 ± 1.60 ml/s, respectively, $^{##}P < 0.01$, Fig. 2B), and the MMF increased by 8.72% (39.41 ± 0.62 ml/L vs. 36.25 ± 1.24 ml/L, respectively, $^{###}P < 0.001$, Fig. 2C). These results suggest that ciprofibrate reversed the CS-induced decline in lung function.

3.3. Ciprofibrate inhibited cigarette smoking-induced airway hypercontraction

To determine whether ciprofibrate affected tracheal contractile function, the response of isolated tracheal rings to acetylcholine (Ach) was examined. The maximum contraction forces of isolated tracheal
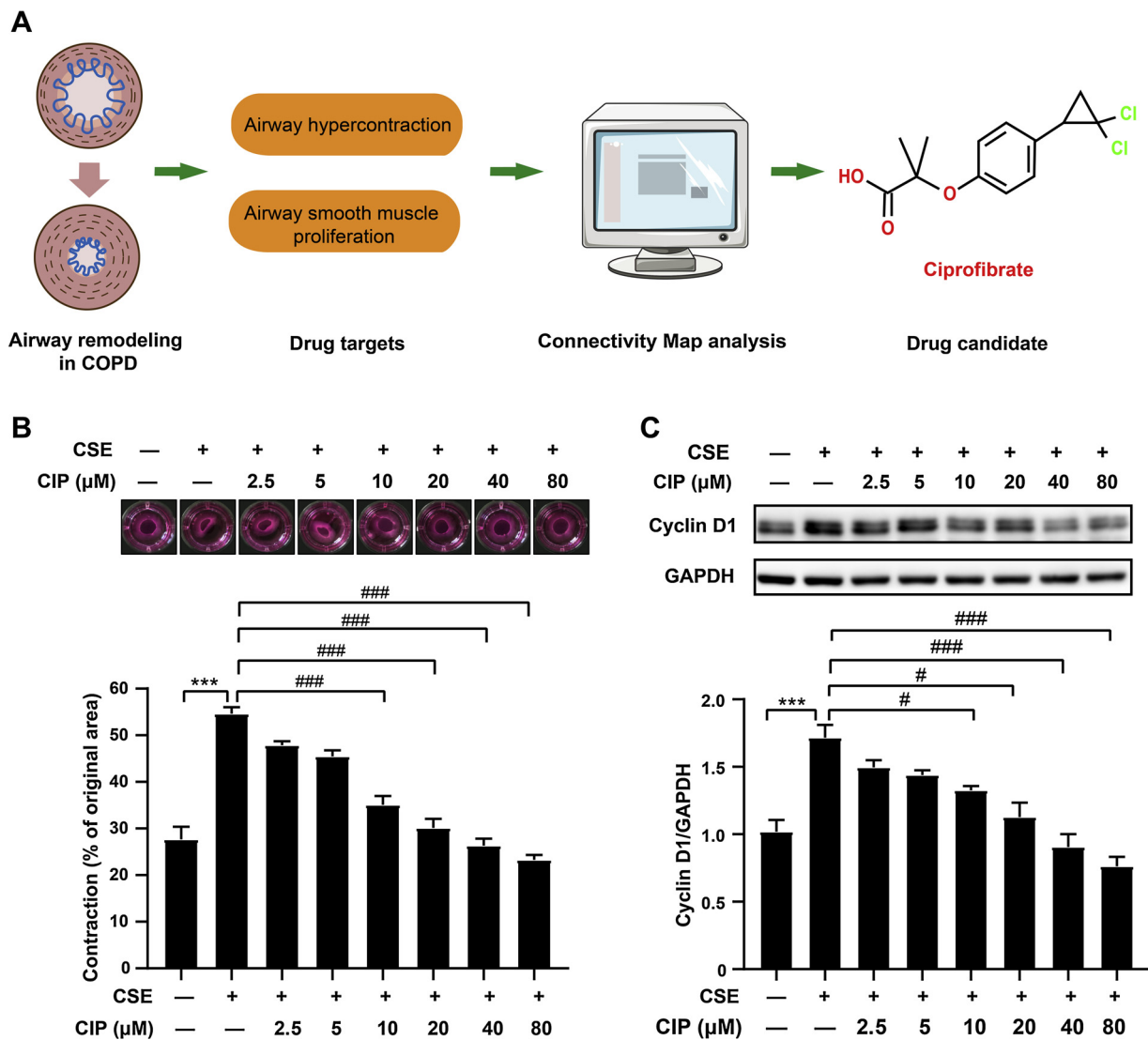
Fig. 1. Identification of ciprofibrate as the drug candidate to attenuate airway remodeling predicted by the Connectivity Map analysis.
(**A**) The paths show that ciprofibrate was identified as a drug candidate by the Connectivity Map analysis. (**B**) Rat airway smooth muscle cell (ASMC) were pre-incubated with different concentrations of ciprofibrate (CIP; 0 μM, 2.5 μM, 5 μM, 10 μM, 20 μM, 40 μM, 80 μM) before stimulation with 0.5% cigarette smoke extract (CSE) for 24 h. The percentage of gel area reduction compared to the original area was evaluated at 24 h. n = 5. Data are mean ± SEM. ***$P < 0.001$ and ###$P < 0.001$. (**C**) Rat ASMC were pre-treated with CIP (0 μM, 2.5 μM, 5 μM, 10 μM, 20 μM, 40 μM, 80 μM) for 2 h followed by stimulation with 0.5% CSE for another 24 h. Protein levels of cyclin D1 in rat ASMC were determined using Western blotting; n = 6. Data are mean ± SEM. ***$P < 0.001$, #$P < 0.05$ and ###$P < 0.001$.

rings in response to 10^{-5} M and 10^{-4} M Ach were significantly higher in the CS-exposed group without ciprofibrate than the clean air-exposed group without ciprofibrate (10^{-5} M Ach: 1.30 ± 0.11 g vs. 0.93 ± 0.10 g, **$P < 0.01$; 10^{-4} M Ach: 1.81 ± 0.21 g vs. 1.06 ± 0.16 g, ***$P < 0.001$, Fig. 3). Notably, ciprofibrate treatment significantly inhibited the maximal contractile force of the isolated tracheal rings in response to 10^{-5} M and 10^{-4} M Ach in the CS-exposed group (10^{-5} M Ach: 1.05 ± 0.14 g vs. 1.30 ± 0.11 g, #$P < 0.05$; 10^{-4} M Ach: 1.32 ± 0.22 g vs. 1.81 ± 0.21 g, ##$P < 0.01$, Fig. 3). The EC_{50} of Ach was not different between the CS-exposed group treated with ciprofibrate and the CS-exposed group without ciprofibrate ($6.06 \pm 1.05 \times 10^{-7}$ M vs. $9.50 \pm 1.16 \times 10^{-7}$ M, #$P > 0.05$). These results indicate that ciprofibrate inhibited CS-induced airway hypercontraction.

3.4. Ciprofibrate attenuated cigarette smoking-induced morphological small airway remodeling

The CS-exposed group without ciprofibrate exhibited airway congestion, epithelial necrosis erosion, smooth muscle proliferation, numerous inflammatory cells in the alveolar walls and spaces, small airway fibrosis and massive disruption of lung structure (Table 1). Chronic ciprofibrate administration improved a number of CS-induced pathological alterations, such as airway occlusion and epithelial necrosis erosion, and special improvements in airway smooth muscle proliferation (1.2 ± 0.3 vs. 2.3 ± 0.3, #$P < 0.05$), inflammatory cell infiltration (1.5 ± 0.2 vs. 2.4 ± 0.2, ##$P < 0.01$) and fibrosis (0.7 ± 0.1 vs. 1.8 ± 0.3, ##$P < 0.01$) (Table 1).

Increased airway wall thickness, the proliferation of ASM and airway matrix deposition are prominent features of airway remodeling in COPD (Jones et al., 2016). Ciprofibrate intervention in the CS-exposed group reduced the bronchiole wall area/basement membrane perimeter (45.25 ± 2.59 μm^2/μm vs. 62.38 ± 2.74 μm^2/μm,

A

B

C
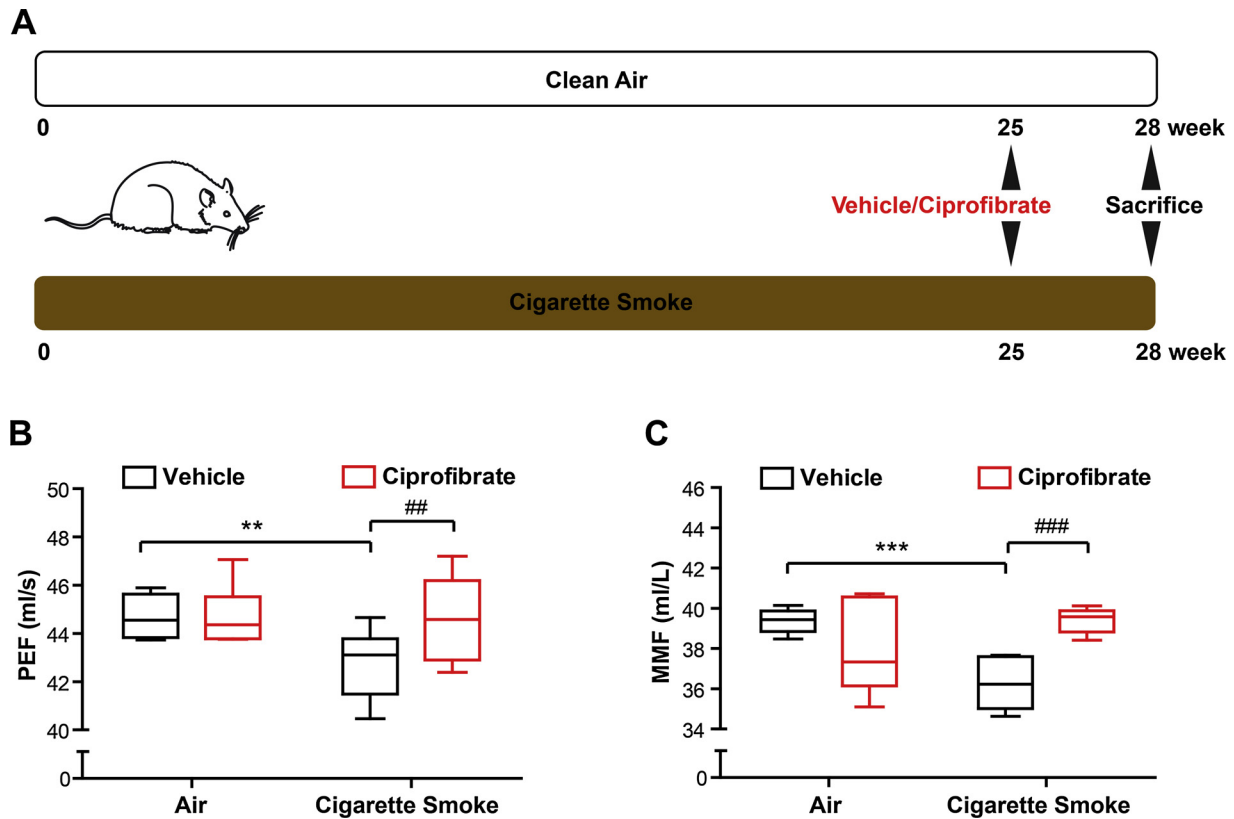
Fig. 2. Ciprofibrate reversed the cigarette smoking-induced decline in lung function.

(**A**) Thirty-two rats were randomly divided into four groups for the challenge (n = 8 each): exposure to clean air or cigarette smoke (CS) for 28 weeks and treated with ciprofibrate (10 mg/kg) or vehicle (1% carboxymethylcellulose sodium) once daily for 4 weeks from the 25th week of exposure. All rats were euthanized after 28 weeks. (**B**) Peak expiratory flow (PEF) and (**C**) maximal mid-expiratory flow curve (MMF) were measured in all groups after 28 weeks. n = 8. Data are presented as box-plots showing the medians and 25th and 75th percentiles and whiskers showing the 10th and 90th percentiles. $**P < 0.01$, $***P < 0.001$, $^{##}P < 0.01$ and $^{###}P < 0.001$.
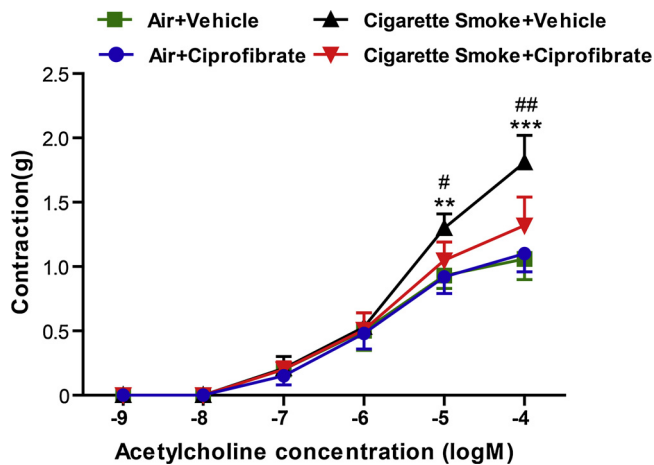
Fig. 3. Ciprofibrate significantly inhibited the maximal contractile of rat isolated tracheal rings response to acetylcholine in cigarette smoke-exposed rats. The contraction force changes of rat isolated tracheal rings response to acetylcholine were measured in four groups. n = 8. Data are mean ± SEM. $**P < 0.01$ and $***P < 0.001$ compared with the clean air-exposed group without ciprofibrate; $^{#}P < 0.05$ and $^{##}P < 0.01$ compared with CS-exposed group without ciprofibrate.

$^{##}P < 0.01$, Fig. 4A-B) and the wall area/total bronchiole area (MA%, 58.62% ± 2.68% vs. 77.63% ± 2.84%, $^{##}P < 0.01$, Fig. 4C) compared to the CS-exposed group without ciprofibrate. Ciprofibrate intervention also reduced the α-SMA staining area of bronchioles/basement membrane perimeter (7.51 ± 0.69 µm²/µm vs. 11.63 ± 0.73 µm²/µm,
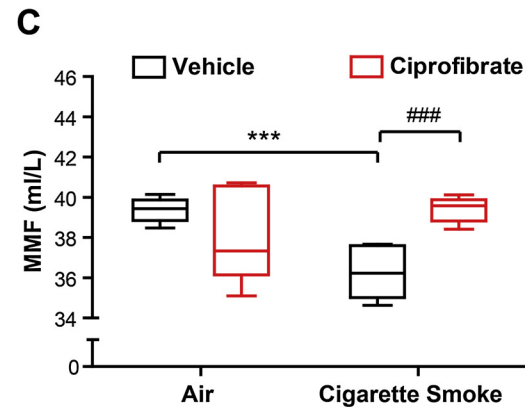
$^{##}P < 0.01$, Fig. 4D-E). Masson staining in the CS-exposed group without ciprofibrate demonstrated a more severe distortion of the lung structure and larger collagen area compared to the clean air-exposed group without ciprofibrate (5.43 ± 0.38 µm²/µm vs. 1.41 ± 0.36 µm²/µm, $***P < 0.001$, Fig. 5). Ciprofibrate treatment in the CS-exposed group decreased the collagen area around bronchioles compared to the untreated CS-exposed group (3.75 ± 0.65 µm²/µm vs. 5.43 ± 0.38 µm²/µm, $^{#}P < 0.05$, Fig. 5B). These results suggest that ciprofibrate ameliorated morphological small airway remodeling, including airway smooth muscle proliferation, in CS-exposed rats.

3.5. Ciprofibrate reduced serum cytokine levels in cigarette smoke-exposed rats

COPD is not just a simple lung disease but a systemic disease that exhibits extensive extrapulmonary damage. A wide variety of inflammatory mediators are increased in COPD, including IL-1β, TNF-α, IL-12p70, IL-17A, IL-18 and IL-33, which amplify the inflammatory process and induce airway structural changes (Churg et al., 2009; Hackett et al., 2014; Kang et al., 2012; Roos and Stampfli, 2017; Xia et al., 2015). We examined the role of ciprofibrate in the CS-induced systemic inflammatory response in rats. The levels of IL-1β, IL-12p70, IL-17A, IL-18 and IL-33 in serum were significantly increased in the CS-exposed group without ciprofibrate compared to the clean air-exposed group without ciprofibrate (Fig. 6A-E). Notably, ciprofibrate treatment reduced the concentrations of IL-1β, IL-12p70, IL-17A, IL-18 and IL-33 in the serum of CS-exposed groups (Fig. 6A-E). However, ciprofibrate did not inhibit TNF-α expression in the serum of the CS-exposed group without ciprofibrate. Notably, there was no difference in TNF-α

Table 1
Pathological scores of rat lung tissue in four groups.

Parameters	Air + Vehicle	Air + Ciprofibrate	Cigarette Smoke + Vehicle	Cigarette Smoke + Ciprofibrate
Airway occlusion	0.8 ± 0.1	0.5 ± 0.2	1.5 ± 0.1**	1.0 ± 0.2#
Epithelial necrosis erosion	0	0	1.4 ± 0.2***	0.8 ± 0.3*#
Goblet cell metaplasia	0.4 ± 0.1	0.3 ± 0.1	0.4 ± 0.1	0.5 ± 0.3
Squamous cell metaplasia	0	0	0	0
Inflammatory cell infiltration	1.2 ± 0.2	1.3 ± 0.3	2.4 ± 0.2**	1.5 ± 0.2##
Fibrosis	0	0	1.8 ± 0.3***	0.7 ± 0.1*##
Smooth muscle proliferation	0.3 ± 0.1	0.2 ± 0.1	2.3 ± 0.3***	1.2 ± 0.3**#
Pigmentation	0	0	0.5 ± 0.1*	0.4 ± 0.2
Emphysema	0	0	2.0 ± 0.3***	1.5 ± 0.2***
Total score	2.7 ± 0.5	2.3 ± 0.7	12.3 ± 1.6***	7.6 ± 1.8*#

Data are mean ± SEM. n = 8.

* $P < 0.05$.

** $P < 0.01$.

*** $P < 0.001$ compared with the clean air-exposed group without ciprofibrate.

\# $P < 0.05$.

\#\# $P < 0.01$ compared with cigarette smoke-exposed group without ciprofibrate.
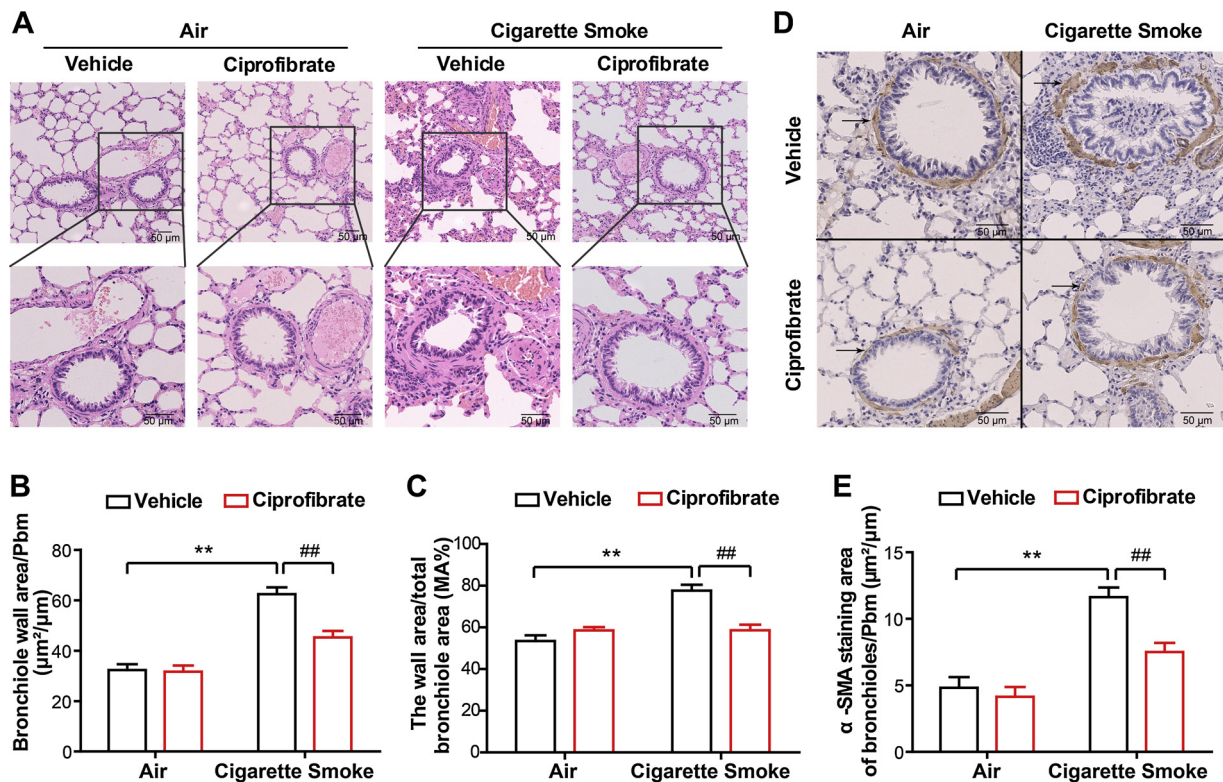
Fig. 4. Ciprofibrate attenuated bronchiole wall area and alpha-smooth muscle actin staining area of bronchioles following cigarette smoke exposure. Representative photomicrographs of lung sections with (**A**) hematoxylin and eosin staining and (**D**) IHC staining of alpha-smooth muscle actin (α-SMA) in each group. (**B**) The bronchiole wall area and (**E**) α-SMA staining area of bronchioles normalized to bronchiole basement membrane perimeter (Pbm) were quantified in the four groups. (**C**) The wall area/total bronchiole area (MA%) was also measured in all groups. n = 8. Data are mean ± SEM. *$P < 0.05$, **$P < 0.01$ and ##$P < 0.01$. Scale bar = 50 μm.

expression in the sera of the CS-exposed group without ciprofibrate and the clean air-exposed group without ciprofibrate (Fig. 6F). These results show that ciprofibrate reduced the systemic inflammatory response in CS-exposed rats.

4. Discussion

In this study, we used the cMap database to repurpose drug candidates with the potential to attenuate the airway remodeling processes associated with COPD. The integration of cMap analysis and literature mining identified ciprofibrate as a drug candidate. The key findings were that ciprofibrate improved cigarette smoke airway remodeling *in*

vitro and *in vivo*. We suggest ciprofibrate as a potential therapeutic drug for airway remodeling in COPD. Our study provides a new strategy to identify drugs for COPD treatment.

Previous studies have demonstrated that single-target drugs treatment for COPD, such as infliximab (an anti-TNF α antibody), canakinumab (an anti-IL-1β antibody) and CNTO6785 (an IL-17A inhibitor), do not benefit COPD patients (Lakshmi et al., 2017). Multiple mechanisms involve in pathological changes of COPD (Lakshmi et al., 2017). Thus, multi-target drug therapy is an important strategy for COPD treatment. cMap database has used for drug repurposing predictions. Intriguing prediction obtained from the cMap-based analysis is to use the antiulcer drug, cimetidine, as a possible therapy in the
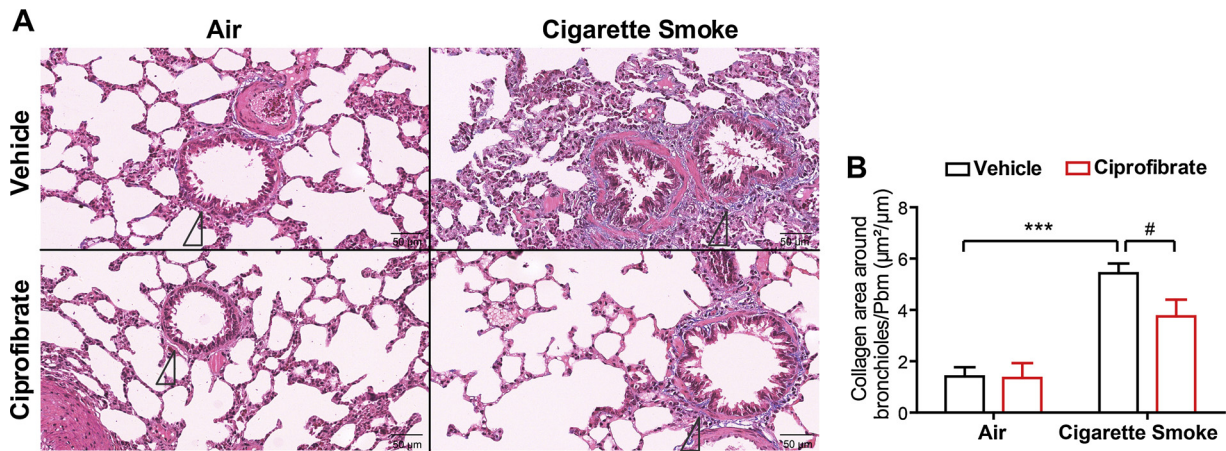
Fig. 5. Ciprofibrate decreased collagen area around bronchioles by cigarette smoking.
(**A**) Representative photomicrographs of lung sections with Masson staining in each group. (**B**) Quantification of the collagen area around bronchioles normalized to bronchiole basement membrane perimeter (Pbm) in all groups. n = 8. Data are mean ± SEM. $^{#}P < 0.05$, $^{**}P < 0.01$ and $^{***}P < 0.001$. Scale bar = 50 μm.

management of lung adenocarcinoma, with *in vitro* and *in vivo* proof-of-concept validation (Qu and Rajpal, 2012). Geldanamycin, a heat shock protein 90 inhibitor, has also been identified and hypothesized to be an anti-mimetic of tobacco effect through cMap analysis using expression profiles of human buccal biopsies from comparing smokers and non-smokers (Qu and Rajpal, 2012). In our study, predicted ciprofibrate attenuated airway remodeling, including airway smooth muscle pro-liferation and airway hypercontraction in CS-exposed rats. Moreover, ciprofibrate had anti-inflammatory properties in CS-exposed rats. In general, these studies have lent confidence to the application of cMap in identifying repurposing candidates. Ciprofibrate, as a multi-target drug predicted by cMap-based analysis, provides a novel idea for the re-purposing of 'old' drugs in COPD treatment.

Cigarette smoke contributes to or exacerbates COPD. Airway hy-percontraction and ASM proliferation are key features of airway re-modeling in COPD. To verify the prediction results, cellular experi-ments were performed. Cigarette smoke extract (CSE) has a significant effect on airway abnormal contractility and proliferation (Chiba et al., 2005; Sathish et al., 2013; Smelter et al., 2010; Wylam et al., 2015; Xu et al., 2012). Our results were consistent with these findings and further demonstrated that ciprofibrate inhibited CSE-induced contraction and proliferation in ASMC. Ciprofibrate inhibits human leukemic cell line HL-60 cells proliferation and affects c-Myb and cyclin D2 expression (Laurora et al., 2003). In hepatoma cell line HepG2 cells, ciprofibrate inhibits cell proliferation by decreasing phosphorylation of c-Myc (Clemencet et al., 2005). Our study indicated that ciprofibrate inhibited ASMC proliferation via restraining cyclin D1 expression. Collectively, these findings suggest that ciprofibrate may have different mechanisms in inhibiting cell proliferation in various cell systems. At present, there are few studies on the inhibition of smooth muscle contraction by ci-profibrate. PPAR-α activation relaxes smooth muscle cells through various pathways in diverse models. Ciprofibrate inhibits homo-cysteine-induced contraction of vascular smooth muscle cells and en-dothelial cells. They may be related to the endothelial nitric oxide
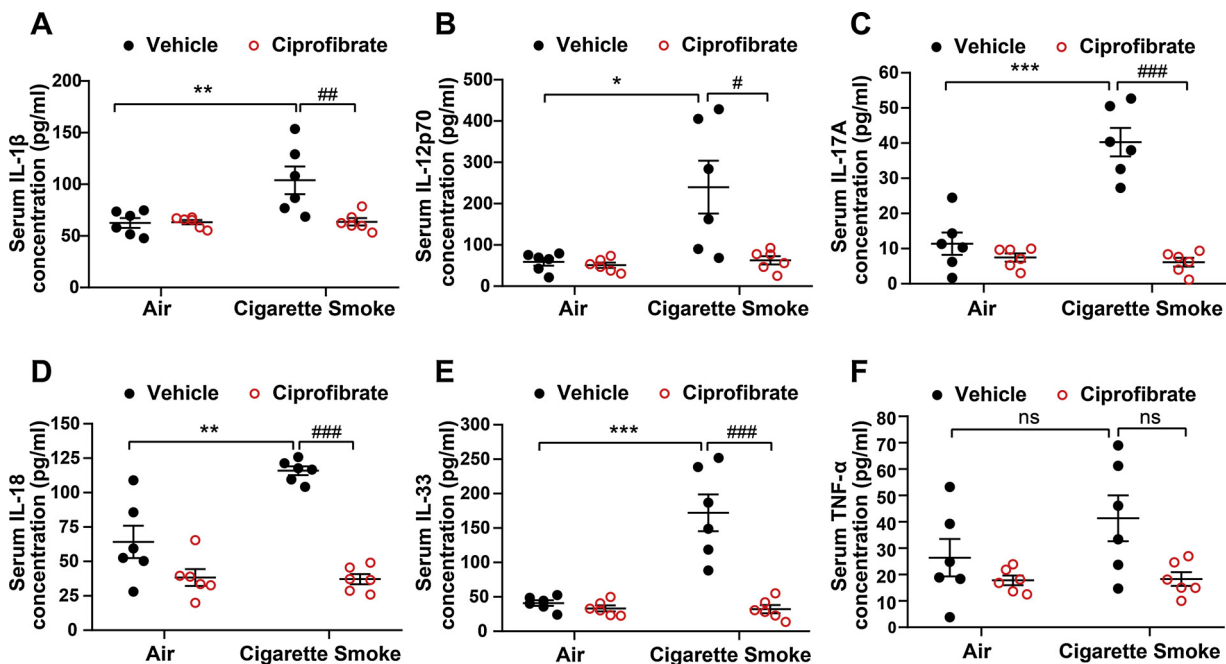
Fig. 6. Ciprofibrate reduced serum cytokine levels in cigarette smoke-exposed rats. (**A**) IL-1β, (**B**) IL-12p70, (**C**) IL-17A, (**D**) IL-18, (**E**) IL-33 and (**F**) TNF-α levels in sera of the four groups were measured using bead-based multi-analyte flow immunoassays. Data are presented as the mean ± SEM with individual data points. n = 6. $^{*}P < 0.05$, $^{**}P < 0.01$, $^{***}P < 0.001$, $^{#}P < 0.05$, $^{##}P < 0.01$ and $^{###}P < 0.001$. ns means no significant difference.

generation (Mujumdar et al., 2002). Clofibrate relaxes the longitudinal smooth muscle of normal mouse distal colon by increasing myosin light-chain phosphatase activity (Azuma et al., 2011). Fenofibrate relaxes thoracic aorta associated with its potency to reduce intracellular calcium in cultured vascular smooth muscle cells (Liu et al., 2012). We used RNA-sequencing to compare the transcriptomic perturbations following ciprofibrate treatment in CS-exposed rats. Ciprofibrate may upregulate the expression of PKA-Cα in rat ASMC. Then, the increase of active PKA-Cα regulates ASMC contractility (Pera and Penn, 2014). This assumption will be verified in our future work.

Previous studies have reported that the PPAR-α activation reduces lipopolysaccharide-induced inflammation (Delayre-Orthez et al., 2005) and acute lung injury (Cuzzocrea, 2006) in mice, which suggest that an activator of PPAR-α may have a beneficial effect on the inflammatory response associated with COPD. We previously reported the effectiveness of long-term CS-exposure on inducing airway remodeling and COPD-like changes based on the pathological and pulmonary function changes that occurred in rat lungs (Zhou et al., 2014a,b). Airway remodeling was proposed as a mechanism that explains many clinical features of persistent bronchial hypercontraction and impaired lung function. The present study established a 28-week CS-exposure model in rats to evaluate the therapeutic effects of chronic ciprofibrate treatment. Surprisingly, ciprofibrate improved the CS-induced decline in lung function, including PEF and MMF as representatives of small airway resistance. Ciprofibrate also ameliorated pathological changes in the lungs, especially the improvement in airway smooth muscle proliferation and the alpha-smooth muscle actin staining area of bronchioles induced by cigarette smoking. Therefore, ciprofibrate treatment may attenuate the smooth muscle proliferation associated with airway remodeling in CS-exposed rats.

COPD is a chronic progressive disease, and the structural changes induced by continuous extrinsic factors result in ASM proliferation and small airway fibrosis, which contribute to the reduced airway lumen, particularly in the face of ongoing airway hypercontraction (Prakash, 2013). Recent works have shown that passive cigarette smoking increased the contractility of isolated tracheal rings to Ach (Guo et al., 2014). Our results are consistent with these findings and further show that ciprofibrate treatment significantly inhibited the maximal contractile force of the isolated tracheal rings in response to Ach in the CS-exposed group. This result may be related to the inhibition of ASM proliferation and contraction to regulate contractile tension in whole isolated tracheal rings. Therefore, ciprofibrate may improve CS-induced airway hypercontraction.

Systemic inflammatory responses are pivotal links in the pathogenesis of COPD, and small airway remodeling is correlated with systemic inflammation (Segal and Martinez, 2018). Ciprofibrate exhibits anti-inflammatory properties (Xu et al., 2005). In this study, ciprofibrate inhibited inflammatory cytokine expression (IL-1β, IL-12p70, IL-17A, IL-18 and IL-33) in the sera of the CS-exposed groups. IL-1β, IL-12p70 and IL-17A play an important role in the pathogenesis of CS-induced small airway remodeling (Churg et al., 2009; Hackett et al., 2014; Roos and Stampfli, 2017). IL-18 induces airway remodeling mediated by IL-17A-dependent mechanisms (Kang et al., 2012). IL-33 relates to airway and systemic inflammation in COPD (Xia et al., 2015). Therefore, ciprofibrate attenuated airway smooth muscle proliferation and small airway fibrosis by the attenuation of systemic inflammation in CS-exposed rats. COPD is characterized by substantial patient-to-patient heterogeneity. Individual patients with COPD vary in the degrees of chronic bronchitis, bronchiolitis and emphysema (Segal and Martinez, 2018). COPD is a highly complex inflammatory disease in which many cytokines and mediators are involved. Previous studies have reported that the concentration of TNF-α in the serum of CS-exposed Sprague-Dawley rats increases dramatically to the highest point at the 4th week. It shows a rapid decline from the 4th to the 24th week and a marked increase after 36 weeks of CS exposure. The cytokines in blood serum vary at different stages of CS exposure (Wang et al., 2018).

No difference in the level of TNF-α in the serum between the clean air-exposed group without ciprofibrate and the CS-exposed group without ciprofibrate at the 28th week in our study may be related to the CS exposure course. Taken together, ciprofibrate may attenuate inflammatory cytokine expression, including IL-1β, IL-12p70, IL-17A, IL-18 and IL-33, which are related to airway remodeling, in the sera of CS-exposed rats. The detailed regulatory mechanism and the biological significance of these cytokines remain to be revealed in the future.

5. Conclusion

We used drug bioinformatics database the cMap to screen for multitarget drugs, such as ciprofibrate, for airway remodeling treatment in COPD. Our study extends our knowledge of the effects of ciprofibrate, a PPAR-α agonist, on a CS-exposed rat model. Our research suggests that ciprofibrate may inhibit CSE-induced rat ASMC contraction and cyclin D1 expression *in vitro* and improve pathological airway smooth muscle proliferation and hypercontraction in CS-exposed rats via the attenuation of serum inflammatory cytokine levels, which are related to airway remodeling, *in vivo*. The administration of ciprofibrate may benefit CS-exposed airway remodeling. Overall, this study provides more direct experimental evidence and a novel idea for COPD treatment.

Author contributions

Bei He, Ming Xu and Youyi Zhang conceived and designed the study. Qian Ke participated in the cell and animal studies and drafted the manuscript. Qinghua Cui helped design and participated in the bioinformatics studies. Bei He and Ming Xu helped in the drafting of the manuscript. Lin Yang and Wenqi Diao participated in animal studies.

Declaration of Competing Interest

The authors have no competing interests to declare.

Appendix A. Supplementary data

Supplementary material related to this article can be found, in the online version, at doi:https://doi.org/10.1016/j.resp.2019.103290.

References

Azuma, Y.T., Nishiyama, K., Morioka, A., Nakajima, H., Takeuchi, T., 2011. Clofibrate relaxes the longitudinal smooth muscle of the mouse distal colon through calcium-mediated desensitisation of contractile machinery. Pharmacology. 88, 65–71. https://doi.org/10.1159/000329418.

Banno, A., Reddy, A.T., Lakshmi, S.P., Reddy, R.C., 2018. PPARs: key regulators of airway inflammation and potential therapeutic targets in asthma. Nucl. Receptor Res. 5. https://doi.org/10.11131/2018/101306.

Barnes, P.J., Burney, P.G., Silverman, E.K., Celli, B.R., Vestbo, J., Wedzicha, J.A., et al., 2015. Chronic obstructive pulmonary disease. Nat. Rev. Dis. Primers 1, 15076. https://doi.org/10.1038/nrdp.2015.76.

Belvisi, M.G., Mitchell, J.A., 2009. Targeting PPAR receptors in the airway for the treatment of inflammatory lung disease. Br. J. Pharmacol. 158, 994–1003. https://doi.org/10.1111/j.1476-5381.2009.00373.x.

Chiba, Y., Murata, M., Ushikubo, H., Yoshikawa, Y., Saitoh, A., Sakai, H., et al., 2005. Effect of cigarette smoke exposure in vivo on bronchial smooth muscle contractility in vitro in rats. Am. J. Respir. Cell Mol. Biol. 33, 574–581. https://doi.org/10.1165/rcmb.2005-0177OC.

Churg, A., Zhou, S., Wang, X., Wang, R., Wright, J.L., 2009. The role of interleukin-1beta in murine cigarette smoke-induced emphysema and small airway remodeling. Am. J. Respir. Cell Mol. Biol. 40, 482–490. https://doi.org/10.1165/rcmb.2008-0038OC.

Clemencet, M.C., Muzio, G., Trombetta, A., Peters, J.M., Gonzalez, F.J., Canuto, R.A., et al., 2005. Differences in cell proliferation in rodent and human hepatic derived cell lines exposed to ciprofibrate. Cancer Lett. 222, 217–226. https://doi.org/10.1016/j.canlet.2004.09.016.

Cosio, M.G.H., Hogg, J.C., Corbin, R., Loveland, M., Dosman, J., Macklem, P.T., 1978. The relations between structural changes in small airways and pulmonary-function tests. N. Engl. J. Med. 298, 1277–1281. https://doi.org/10.1056/NEJM197806082982303.

Cuzzocrea, S., 2006. Peroxisome proliferator-activated receptors and acute lung injury. Curr. Opin. Pharmacol. 6, 263–270. https://doi.org/10.1016/j.coph.2006.01.008.

Dekkers, B.G., Racke, K., Schmidt, M., 2013. Distinct PKA and Epac compartmentalization in airway function and plasticity. Pharmacol. Ther. 137, 248–265. https://doi.org/10.1016/j.pharmthera.2012.10.006.

Delayre-Orthez, C., Becker, J., Guenon, I., Lagente, V., Auwerx, J., Frossard, N., et al., 2005. PPARalpha downregulates airway inflammation induced by lipopolysaccharide in the mouse. Respir. Res. 6, 91. https://doi.org/10.1186/1465-9921-6-91.

Guo, Y., Zhang, Y., Shen, N., Zhou, Y., Zhang, Y., Wupuer, H., et al., 2014. Effects of one month treatment with propranolol and metoprolol on the relaxant and contractile function of isolated trachea from rats exposed to cigarette smoke for four months. Inhal. Toxicol. 26, 271–277. https://doi.org/10.3109/08958378.2014.885098.

Hackett, T.L., Shaheen, F., Zhou, S., Wright, J.L., Churg, A., 2014. Fibroblast signal transducer and activator of transcription 4 drives cigarette smoke-induced airway fibrosis. Am. J. Respir. Cell Mol. Biol. 51, 830–839. https://doi.org/10.1165/rcmb.2013-0369OC.

Herbert, J.M., Bernat, A., Chatenet-Duchene, L., 1999. Effect of ciprofibrate on fibrinogen synthesis in vitro on hepatoma cells and in vivo in genetically obese Zucker rats. Blood Coagul. Fibrinolysis 10, 239–244.

Jones, R.L., Noble, P.B., Elliot, J.G., James, A.L., 2016. Airway remodelling in COPD: it's not asthma!. Respirology 21, 1347–1356. https://doi.org/10.1111/resp.12841.

Kang, M.J., Choi, J.M., Kim, B.H., Lee, C.M., Cho, W.K., Choe, G., et al., 2012. IL-18 induces emphysema and airway and vascular remodeling via IFN-gamma, IL-17A and IL-13. Am. J. Respir. Crit. Care Med. 185, 1205–1217. https://doi.org/10.1164/rccm.201108-1545OC.

Lahousse, L., Verhamme, K.M., Stricker, B.H., Brusselle, G.G., 2016. Cardiac effects of current treatments of chronic obstructive pulmonary disease. Lancet Respir. Med. 4, 149–164. https://doi.org/10.1016/s2213-2600(15)00518-4.

Lakshmi, S.P., Reddy, A.T., Reddy, R.C., 2017. Emerging pharmacological therapies for COPD. Int. J. Chron. Obstruct. Pulmon. Dis. 12, 2141–2156. https://doi.org/10.2147/COPD.S121416.

Lamb, J., Crawford, E.D., Peck, D., Modell, J.W., Blat, I.C., Wrobel, M.J., et al., 2006. The Connectivity Map: using gene-expression signatures to connect small molecules, genes, and disease. Science. 313, 1929–1935. https://doi.org/10.1126/science.1132939.

Laurora, S., Pizzimenti, S., Briatore, F., Fraioli, A., Maggio, M., Reffo, P., et al., 2003. Peroxisome proliferator-activated receptor ligands affect growth-related gene expression in human leukemic cells. J. Pharmacol. Exp. Ther. 305, 932–942. https://doi.org/10.1124/jpet.103.049098.

Li, S., Yang, B., Du, Y., Lin, Y., Liu, J., Huang, S., et al., 2018. Targeting PPARalpha for the treatment and understanding of cardiovascular diseases. Cell. Physiol. Biochem. 51, 2760–2775. https://doi.org/10.1159/000495969.

Liu, A., Yang, J., Huang, X., Xiong, J., Wong, A.H., Chang, L., et al., 2012. Relaxation of rat thoracic aorta by fibrate drugs correlates with their potency to disturb intracellular calcium of VSMCs. Vascul. Pharmacol. 56, 168–175. https://doi.org/10.1016/j.vph.2012.01.003.

Mujumdar, V.S., Tummalapalli, C.M., Aru, G.M., Tyagi, S.C., 2002. Mechanism of constrictive vascular remodeling by homocysteine: role of PPAR. Am. J. Physiol., Cell Physiol. 282, C1009–1015. https://doi.org/10.1152/ajpcell.00353.2001.

Pera, T., Gosens, R., Lesterhuis, A.H., Sami, R., van der Toorn, M., Zaagsma, J., et al., 2010. Cigarette smoke and lipopolysaccharide induce a proliferative airway smooth muscle phenotype. Respir. Res. 11, 48. https://doi.org/10.1186/1465-9921-11-48.

Pera, T., Penn, R.B., 2014. Crosstalk between beta-2-adrenoceptor and muscarinic acetylcholine receptors in the airway. Curr. Opin. Pharmacol. 16, 72–81. https://doi.org/10.1016/j.coph.2014.03.005.

Prakash, Y.S., 2013. Airway smooth muscle in airway reactivity and remodeling: what have we learned? Am. J. Physiol. Lung Cell Mol. Physiol. 305, L912–933. https://doi.org/10.1152/ajplung.00259.2013.

Pushpakom, S., Iorio, F., Eyers, P.A., Escott, K.J., Hopper, S., Wells, A., et al., 2018. Drug repurposing: progress, challenges and recommendations. Nat. Rev. Drug Discov. 18, 41–58. https://doi.org/10.1038/nrd.2018.168.

Qu, X.A., Rajpal, D.K., 2012. Applications of connectivity map in drug discovery and development. Drug Discov. Today 17, 1289–1298. https://doi.org/10.1016/j.drudis.2012.07.017.

Rabe, K.F., Watz, H., 2017. Chronic obstructive pulmonary disease. Lancet (London, England). 389, 1931–1940. https://doi.org/10.1016/s0140-6736(17)31222-9.

Reinhardt, A.K., Bottoms, S.E., Laurent, G.J., McAnulty, R.J., 2005. Quantification of collagen and proteoglycan deposition in a murine model of airway remodelling. Respir. Res. 6, 30. https://doi.org/10.1186/1465-9921-6-30.

Roos, A.B., Stampfli, M.R., 2017. Targeting interleukin-17 signalling in cigarette smoke-induced lung disease: mechanistic concepts and therapeutic opportunities. Pharmacol. Ther. 178, 123–131. https://doi.org/10.1016/j.pharmthera.2017.04.001.

Sathish, V., Vanoosten, S.K., Miller, B.S., Aravamudan, B., Thompson, M.A., Pabelick, C.M., et al., 2013. Brain-derived neurotrophic factor in cigarette smoke-induced airway hyperreactivity. Am. J. Respir. Cell Mol. Biol. 48, 431–438. https://doi.org/10.1165/rcmb.2012-0129OC.

Segal, L.N., Martinez, F.J., 2018. Chronic obstructive pulmonary disease subpopulations and phenotyping. J. Allergy Clin. Immunol. 141, 1961–1971. https://doi.org/10.1016/j.jaci.2018.02.035.

Smelter, D.F., Sathish, V., Thompson, M.A., Pabelick, C.M., Vassallo, R., Prakash, Y.S., 2010. Thymic stromal lymphopoietin in cigarette smoke-exposed human airway smooth muscle. J. Immunol. 185, 3035–3040. https://doi.org/10.4049/jimmunol.1000252. Baltimore, Md. : 1950.

Tam, A., Churg, A., Wright, J.L., Zhou, S., Kirby, M., Coxson, H.O., et al., 2016. Sex differences in airway remodeling in a mouse model of chronic obstructive pulmonary disease. Am. J. Respir. Crit. Care Med. 193, 825–834. https://doi.org/10.1164/rccm.201503-0487OC.

Tanaka, T., Ishihara, T., Sugizaki, T., Kobayashi, D., Yamashita, Y., Tahara, K., et al., 2013. Mepenzolate bromide displays beneficial effects in a mouse model of chronic obstructive pulmonary disease. Nat. Commun. 4, 2686. https://doi.org/10.1038/ncomms3686.

Turpin, G., Bruckert, E., 1996. Efficacy and safety of ciprofibrate in hyperlipoproteinaemias. Atherosclerosis(Suppl: S83-87). https://doi.org/10.1016/0021-9150(96)05861-3.

Tzeng, T.F., Tzeng, Y.C., Cheng, Y.J., Liou, S.S., Liu, I.M., 2015. The ethanol extract from Lonicera japonica thunb. Regresses nonalcoholic steatohepatitis in a methionine- and choline-deficient diet-fed animal model. Nutrients 7, 8670–8684. https://doi.org/10.3390/nu7105423.

Wang, G., Mohammadtursun, N., Sun, J., Lv, Y., Jin, H., Lin, J., et al., 2018. Establishment and evaluation of a rat model of sidestream cigarette smoke-induced chronic obstructive pulmonary disease. Front. Physiol. 9, 58. https://doi.org/10.3389/fphys.2018.00058.

Wylam, M.E., Sathish, V., VanOosten, S.K., Freeman, M., Burkholder, D., Thompson, M.A., et al., 2015. Mechanisms of cigarette smoke effects on human airway smooth muscle. PLoS One 10, e0128778. https://doi.org/10.1371/journal.pone.0128778.

Xia, J., Zhao, J., Shang, J., Li, M., Zeng, Z., Zhao, J., et al., 2015. Increased IL-33 expression in chronic obstructive pulmonary disease. Am. J. Physiol. Lung Cell Mol. Physiol. 308, L619–627. https://doi.org/10.1152/ajplung.00305.2014.

Xu, G.N., Yang, K., Xu, Z.P., Zhu, L., Hou, L.N., Qi, H., et al., 2012. Protective effects of anisodamine on cigarette smoke extract-induced airway smooth muscle cell proliferation and tracheal contractility. Toxicol. Appl. Pharmacol. 262, 70–79. https://doi.org/10.1016/j.taap.2012.04.020.

Xu, J., Storer, P.D., Chavis, J.A., Racke, M.K., Drew, P.D., 2005. Agonists for the peroxisome proliferator-activated receptor-alpha and the retinoid X receptor inhibit inflammatory responses of microglia. J. Neurosci. Res. 81, 403–411. https://doi.org/10.1002/jnr.20518.

Yue, H., Yan, W., Ji, X., Gao, R., Ma, J., Rao, Z., et al., 2017. Maternal exposure of BALB/c mice to indoor NO2 and allergic asthma syndrome in offspring at adulthood with evaluation of DNA methylation associated Th2 polarization. Environ. Health Perspect. 125, 097011. https://doi.org/10.1289/EHP685.

Zhou, Y., Xu, M., Zhang, Y., Guo, Y., Zhang, Y., He, B., 2014a. Effects of long-term application of metoprolol and propranolol in a rat model of smoking. Clin. Exp. Pharmacol. Physiol. 41, 708–715. https://doi.org/10.1111/1440-1681.12261.

Zhou, Y., Zhang, Y., Guo, Y., Zhang, Y., Xu, M., He, B., 2014b. beta2-Adrenoceptor involved in smoking-induced airway mucus hypersecretion through beta-arrestin-dependent signaling. PLoS One 9, e97788. https://doi.org/10.1371/journal.pone.0097788.